FAILURE PROCESS IN RC BEAMS SHEAR-STRENGTHENED WITH FRP IN HOGGING MOMENT ZONE

P.C. Liu[1], G.M. Chen[2] and J.F. Chen[3]

[1]School of the Civil and Transportation Engineering,
Guangdong University of Technology, Guangzhou, China
[2]School of the Civil and Transportation Engineering,
Guangdong University of Technology, Guangzhou, China
Email: hustcgm@163.com
[3]School of Natural and Built Environment,
Queen's University Belfast, Belfast BT9 5AG, UK

Keywords: FRP, failure process, RC beams, shear strength, hogging moment zone

Abstract

RC beams shear-strengthened with externally bonded FRP usually fail in shear either by FRP debonding or by FRP rupture. The failure processes of the beams with different strengthening configurations and subjected to different load conditions are different. Following our previous analytical study on progressive failure in RC beams shear-strengthened with FRP strips in sagging moment zone, this paper presents an analytical study on the failure processes in RC beams shear-strengthened with FRP in hogging moment zone. Next, the closed-formed solution for complete debonding failure process is presented first , based on which the contribution of the shear-strengthening FRP to the shear capacity of the beam is quantified. The validity of the analytical solution was verified by comparing its predictions with the numerical results from a finite element analysis.

1. Introduction

The shear resistance of reinforced concrete (RC) beams can be enhanced by externally bonding of fiber-reinforced polymer (FRP). The FRP reinforcement can be bonded around the whole beam (complete wrapping), or two sides and soffit of the beam (U-jacketing), or just to two sides of the beam (side bonding) (Teng et al. 2002) [1]. During the past two decades, there is extensive research on the RC beams shear-strengthened with FRP; however, some aspects of the behavior of the strengthened beams are still not very clear. Such aspects include the effect of beam size, the shear interaction between different components of the strengthened beams, and the effect of shear span-to-depth ratio.

The failure modes of RC beams shear-strengthened by FRP can be different for the different strengthening scenarios. For the beams shear-strengthened by FRP side strips and U-strips, FRP debonding is the governing failure mode, and for the beams shear-strengthened by FRP wraps, FRP rupture is the governing failure mode. Chen and Teng (2003a,b) [2,3] presented different shear strength models for the above two typical failure modes respectively with the assumption of one critical diagonal crack (CDC). Monti et al. (2004) [4] first presented the relationship between the effective stress of FRP and the shear crack width for FRP side strips, U-strips and FRP wraps based on simplifying assumptions (e.g. slips at the two sides of the critical shear crack are equal). Chen et al. (2010) [5] carried out a numerical study on the contribution of steel stirrups as the CDC widens. Chen et al. (2012) [6] presented a more accurate close-formed solution for the full-range debonding process of FRP side strips and U strips based on which the development of FRP shear contribution as the CDC widens can be quantified. Based on Chen et al. (2010, 2012), Chen et al (2013) [7] developed a shear strength model capable of considering the shear interaction between external FRP strips and internal steel stirrups.

However, Monti et al.'s (2004) [4] and Chen et al.'s (2012) [6] solution are corresponding to the situation in sagging moment zone, the shear strengthening in hogging moment zone is common situation in real practice, such as continuous beams and cantilever beams. These two kinds of beams have different boundary conditions and thus the contributions of FRP can be different as well. The experimental studies also showed that there are significant differences in shear strengthening effect between these two kinds of beams (Higgins et al. 2012) [8].

Against the above background, this paper presents a close-form analytical solution for the shear contribution of FRP side strips, U-jackets and wraps in hogging moment zone. Following Chen et al. (2012) [6], the close-form solution is based on the assumption that there is a linearly softening bond-slip relationship in FRP-to-concrete bonded interface for full-range FRP-to-concrete bonded joints (Fig. 1). Also, the analytical solution assumes a linear critical shear crack shape which makes the predictions of shear contribution of FRP most conservative (Chen et al. 2017a) [9]. The close-form analytical solution was then verified by comparing its solutions with the predictions of finite element (FE) model.

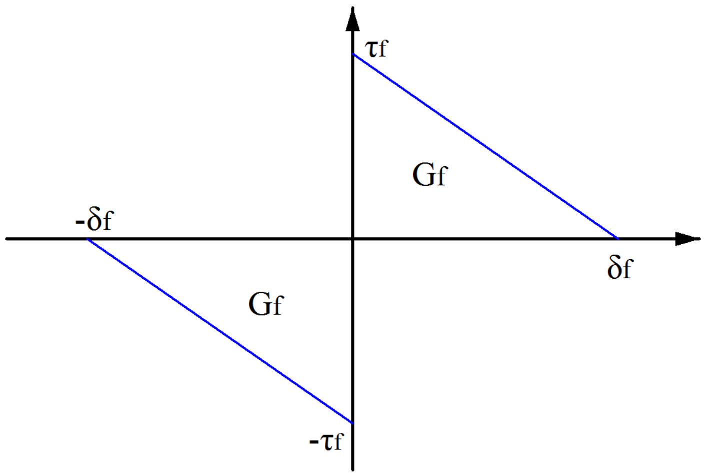

Figure 1. Linearly softening bond-slip model.

2. Analytical model

2.1. Basic equations and assumptions

As in Chen et al. (2012) [6], it is assumed in this study that there is only one critical shear crack at an angle of θ to the horizontal axis of the strengthened and the angle between the FRP fiber and the horizontal axis is termed as β. Other details of the assumptions adopted in developing the solution can be found in Chen et al. (2017b) [10].

The shear contribution of FRP can be evaluated as in Chen and Teng (2003a,b) [2,3]:

$$V_f = 2 f_{f,e} t_f w_f \frac{h_{f,e}(\cot\theta + \cot\beta)\sin\beta}{s_f} \tag{1}$$

where $f_{f,e}$ is the average effective stress in FRP strips, t_f is the thickness of FRP strips, w_f is the width of an individual FRP strip perpendicular to the fiber direction, s_f is the center-to-center spacing of neighboring FRP strips measured along the longitudinal axis, the relationship between w_f and s_f can be expressed as $w_f = s_f \sin\beta$. The development of the effective stress in FRP with shear crack width can be expressed as:

$$f_{f,e} = \frac{\int_0^{h_{f,e}} \sigma(z)dz}{h_{f,e}} \tag{2}$$

Due to limit of space of conference paper, the detailed derivation of the solutions for FRP side strips and FRP U-strips can be found in Chen et al. (2017b) [10] and only the main solutions of the FRP wraps are presented below.

2.2. Failure process of FRP wraps

The failure process for the case of thick concrete cover with $h_t \csc\beta < a_u$ can be divided into four stages: (a) softening stage with $0 \le L_m \le a_u$, (b) debonding stage with $a_u \le L_m \le (h_{f,e} + 0.1d)\csc\beta$, (c) hardening stage with $w_{e,u} \le w_e \le w_{e,r}$, (d) rupture stage with $w_e \ge w_{e,r}$. The solution for other situation and detailed derivation can be found in Chen et al. (2017b) [10].

(a) Softening stage with $0 \le L_m \le a_u$ (Fig. 2a):
The solution for this stage is just like the same stage of FRP side strips, see Chen et al. (2017b)[10] for details.

(b) Debonding stage with $a_u \le L_m \le (h_{f,e} + 0.1d)\csc\beta$ (Fig. 2b to 2d)
With L_m increasing, the rightmost FRP fiber debond first and then the debonding moves towards left. This stage can be divided into 2 partial debonding stage: (I) with $a_u \le L_m \le h_t \csc\beta$ (Fig. 3b) and (II) partial debonding stage with $h_t \le L_m \le (h_{f,e} + 0.1d)\csc\beta$ (Fig. 3c and Fig. 3d). At the end of the partial debonding stage (II) (Fig. 3d), the crack end width $w_e = w_{e,u}$. The D_{frp} and w_e can be obtained by:

$$D_{frp} = (\frac{\pi}{4}\frac{h_{df}}{h_{f,e}} + \frac{h_{f,e} - h_{df}}{h_{f,e}}) \tag{3}$$

$$w_e = \frac{2\delta_f[1 + \lambda(L_m - a_u)]}{\sin(\theta + \beta)} \tag{4}$$

The crack end width at the end of this stage (Fig. 2d) is:

$$w_e = w_{e,u} = \frac{2\delta_f + \delta_f \lambda[(h_{f,e} + h_t + h_b)\csc\beta - 2a_u]}{\sin(\theta+\beta)} \tag{5}$$

In Eqs (3)-(5), a_u is the effective bond length of FRP, L_m is the maximum mobilized length, h_{df} is the vertical distance from the crack tip and point “D” (Fig. 2b), δ_f is the maximum interfacial shear stress of the FRP-to-concrete bonded interface and λ is a dimensionless constant defined to qualify a_u(see Chen et al. (2017b) for more details).

(c) Hardening stage with $w_{e,u} \le w_e \le w_{e,r}$ (Fig. 3e and 3f)

The hardening stage starts when the softening front (where $\tau = \tau_f$ and $\delta = \delta_f$) the rightmost FRP fiber just reaches the bottom edge of the FRP wraps and $w_e = w_{e,u}$ at this time (Fig. 3d), it ends when the rightmost FRP fiber begins to rupture at the crack end width $w_e = w_{e,r}$ (Fig. 3f). The $w_{e,r}$ and D_{frp} can be obtained by:

$$w_{e,r} = \frac{2\delta_f + \dfrac{f_f[(h_t + h_{f,e} + h_c)\csc\beta - \dfrac{2}{\lambda}\arcsin(\dfrac{\tau_f}{\lambda t_f f_f})]}{E_f}}{\sin(\theta+\beta)} \tag{6}$$

$$D_{frp} = \frac{\pi}{4}\frac{h_{df}}{h_{f,e}} + \frac{h_{f,e} - h_{db} - h_{df}}{h_{f,e}} + \frac{w_e - w_{e,u}}{w_e} + \frac{K(w_e - w_{e,u})^2}{2w_e\sigma_b} \tag{7}$$

where $\sigma_b = \frac{\tau_f}{\lambda t_f} = \sqrt{\frac{2G_f E_f}{t_f}}$ is the bond stress of FRP-to-concrete interface without anchorage, h_{db} is the vertical distance between “H” point and the crack end (Fig. 2e), and $K = \dfrac{f_f - \sigma_b}{w_{e,r} - w_{e,u}}$.

(d) Rupture stage with $w_e \ge w_{e,r}$ (Fig. 3g)

The rupture stage starts when the rightmost FRP begins to rupture (Fig. 3g). During this stage, D_{frp} and w_e can be determined by:

$$D_{frp} = (\frac{\pi}{4}\frac{h_{df}}{h_{f,e}} + \frac{h_{f,e} - h_{rp} - h_{db} - h_{df}}{h_{f,e}}) + \frac{w_{e,r} - w_{e,u}}{w_e} + \frac{K(w_{e,r} - w_{e,u})^2}{2w_e\sigma_0} \tag{8}$$

$$w_e = \frac{h_{f,e}}{h_{f,e} - h_r - h_{db}} w_{e,u} = \frac{h_{f,e}}{h_{f,e} - h_r} w_{e,r} \tag{9}$$

where h_r is the vertical distance between “R” point and the crack end (Fig. 2g)

3. Verification of the analytical solution

To verify the analytical solutions, its prediction is compared with FE predictions as in Chen et al. (2012) [6]. In the FE model, the continuous FRP sheet is represented by 20 separate FRP strips, and the material parameters are the same as what is presented in Chen et al. (2012) [6] expect that the beam has a T-section and FRP strips can not be extended to the beam top. All fibers are assumed to be oriented vertically (β=90°) and the angle of shear crack θ=45°. For side strips and U-jackets, the effective height of the crack $0.9d$=300mm, h_f=100mm (height of bean flange) and h_c=50mm (height of concrete cover, defined as the vertical distance from the centroid of tension bars to beam top), as a result, $h_{f,e}=0.9d+ h_c - h_f$ =250mm. The thickness of FRP t_f=0.11mm.

Fig. 3 shows the relationship between crack end width w_e and the FRP shear contribution V_f. The curves of analytical solution are almost identical to FEM predictions for the ascending stage, with the percentage differences between peak V_f and corresponding w_e being no more than 2% (see Chen et al. (2017b) [11] for details). The FE model predicts stepwise drops after the V_f - w_e curve peaks because each drop represents the rupture (FRP wraps) or complete debonding of one strip (FRP side strips/U-strips). For U-jackets and wraps, the curve of analytical solution generally passes the mid-point of each stepwise drop of FEM solution in descending stage. For side strips, the FEM solution drops in a more abrupt way than the analytical solution, but it has insignificant effect with the accuracy of analytical solution, as explained in Chen et al. (2017b) [11].

4. Conclusions

This paper presents a closed-form analytical solution for the whole failure process of FRP side strips, U-jackets and wraps in RC beams in the hogging moment zone, it is based on the assumption of linear critical shear crack shape and the linear bond-slip relationship for FRP-to-concrete bonded interface. The analytical solution is validated by comparing with the FE predictions. One of the major benefits of this close-form solution is that it can be directly used to evaluate the shear contribution of FRP in hogging moment zone as the critical shear crack widens, and it can also be used to evaluate the possible shear interaction between FRP, concrete and steel stirrups in RC beams.

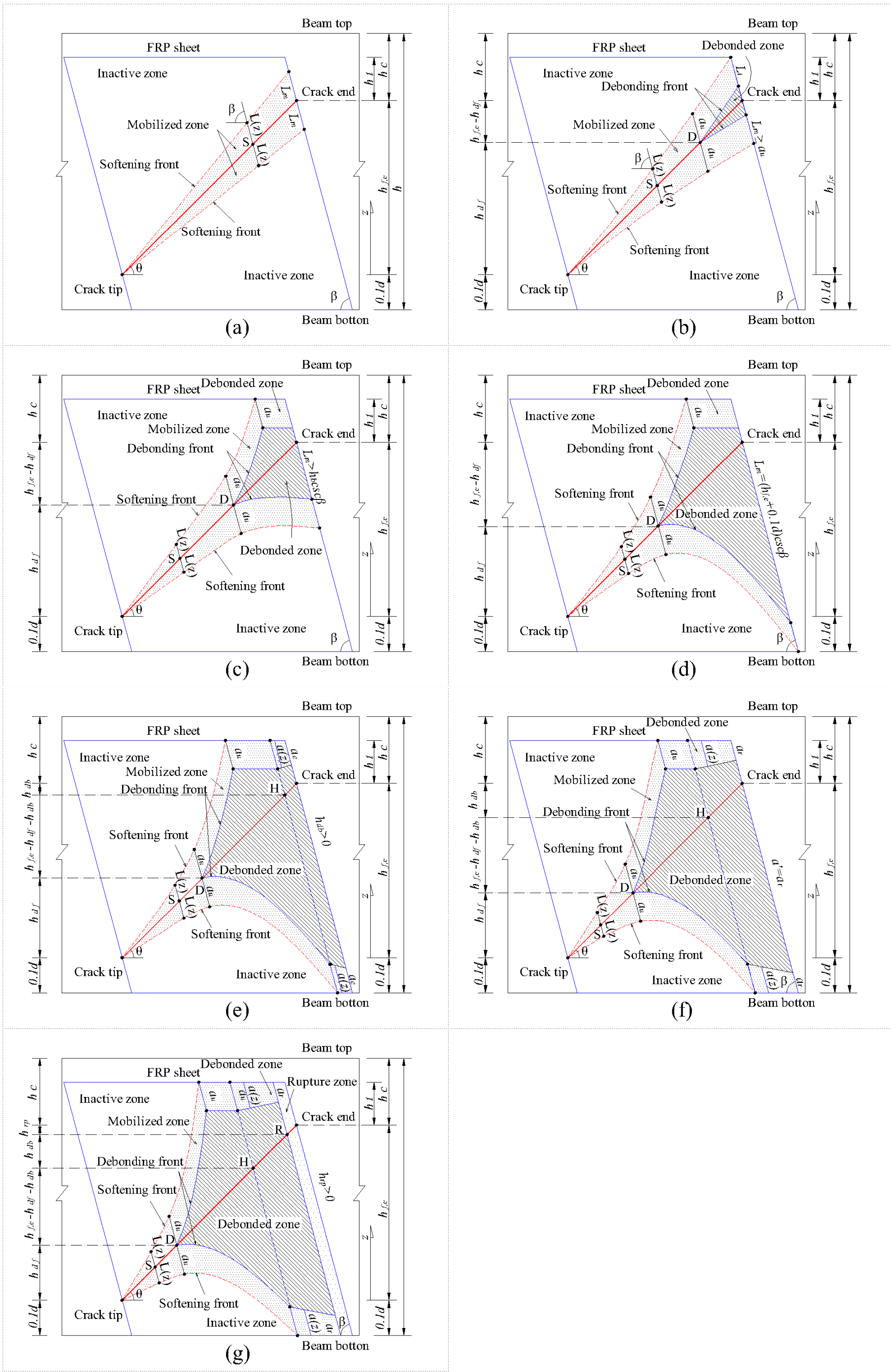

Figure 2. Failure process of FRP wrap for a thick concrete cover.

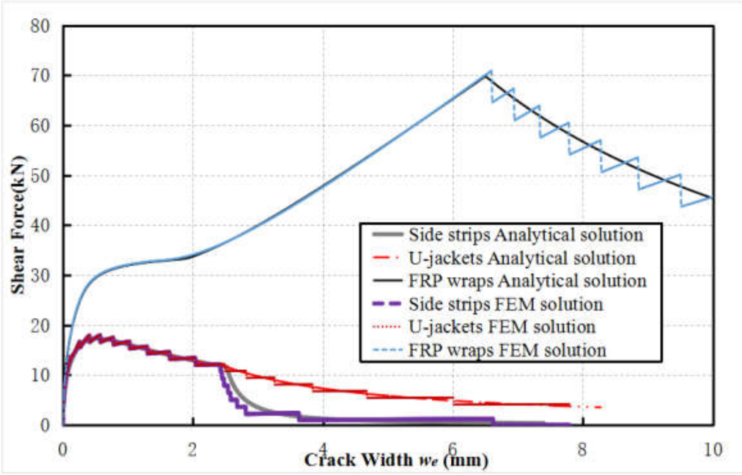

Figure 3. Analytical solution versus FE predictions.

Acknowledgments

The authors acknowledge the financial support received from the National Natural Science Foundation of China (Project Nos. 51108097, 51378130, 51678161) and Guangdong Natural Science Foundation (Project No. S2013010013293).

References

[1] Teng, J.G, Chen, J.F, S.T Smith, L Lam, FRP: strengthened RC structures.
[2] Chen, J.F. and Teng, J.G. (2003). Shear capacity of FRP strengthened RC beams: fibre reinforced polymer rupture, *Journal of Structural Engineering*, ASCE, 129(5), 615-625.
[3] Chen, J.F., Teng, J.G.(2003b). Shear capacity of FRP-strengthened RC beams: FRP debonding. *Construction and Building Materials* 17: 27-41
[4] Monti, G., Santinelli, F. and Liotta, M.A. (2004). Mechanics of FRP shear strengthening of RC beams, Proceedings, *11th European Conference on Composite Materials* (ECCM 11), Rhodes, Greece, May.
[5] Chen, G.M., Teng, J.G., Chen, J.F. and Rosenboom, O. A. (2010). Interaction between steel stirrups and shear-strengthening FRP strips in RC beams, *Journal of Composites for Construction*, ASCE, 14(5), 498-509.
[6] Chen, G.M., Teng, J.G. and Chen, J.F. (2012). Process of debonding in RC beams shear-strengthened with FRP U strips or side strips, *International Journal of Solids and Structures*, 46(10), 1266-1282.
[7] Chen, G.M., Teng, J.G. and Chen, J.F. (2013). Shear strength model for FRP-strengthened RC beams with adverse FRP-steel interaction, *Journal of Composites for Construction*, ASCE, 17(1), 50-66.
[8] Higgins, C., Williams, G.T., Mitchell, M.M., Dawson, M.R. and Howell, D. (2012). Shear strength of reinforced concrete girders with carbon fiber-reinforced polymer: experimental results, *ACI Structural Journal*. 109(6), 805-814
[9] G.M. Chen, S.W. Li, Fernando, D., P.C. Liu and J.F. Chen (2017a). Full-range failure behaviour in RC beams shear-strengthened with FRP wraps, *International Journal of Solids and Structures*, Submitted
[10] G.M. Chen, P.C. Liu, Fernando, D. and J.F. Chen (2017b). Full-range failure process in RC beams shear-strengthened with FRP in hogging moment zone: An analytical solution, under preparation.